Bozok J Eng Arch, 2024; 3(2) 110-124
DOI: 10.70700/bjea.1586153

Bozok
Journal of Engineering and Architecture

e-ISSN: 3023-4298
Research Article

Heat transfer in two-zone thick-walled pipes with axial varying periodic temperature boundary condition

Ali ATEŞ[1] *

[1] *Sinop University, Faculty of Engineering and Architecture, Department of Mechanical Engineering, Sinop, Türkiye*

ARTICLE INFO

Article History:

Received
15.11.2024
Accepted
10.12.2024
Published
31.12.2024

Keywords:

Transient conjugate heat transfer
Axially periodic temperature
Thick walled pipes
Heat transfer to upstream region

ABSTRACT

The conjugate heat transfer in thick-walled pipes is investigated by also considering axial heat conduction. The problem considers a two-zone infinite pipe. There is a constant outer wall temperature boundary condition in the upstream region of the pipe. In the downstream region, the outer wall temperature is assumed to vary periodically in the axial direction spatially. This problem, where the flow is assumed to be laminar, is solved numerically by the finite difference method. The effects of the basic parameters of wall thickness ratio, Peclet number, wall-fluid thermal conductivity coefficient ratio and wall-fluid thermal diffusivity coefficient ratio on the interface heat flux are investigated. The effects of the axial dimensionless frequency on the results are also taken into account in the studies. The results obtained are highly dependent on the parametric values. It is observed that the wall thickness ratio is more effective than the other parametric values. In addition, it can be said that the pipe wall and fluid axial conduction cause heat transfer to upstream region at a non-negligible scale.

Eksenel yönde periyodik olarak değişen sıcaklık sınır şartıyla iki bölgeli kalın cidarlı borularda ısı transferi

MAKALE BİLGİSİ

Makale Tarihleri:

Geliş tarihi
15.11.2024
Kabul tarihi
10.12.2024
Yayın tarihi
31.12.2024

Anahtar Kelimeler:

Geçici rejim birleşik ısı transferi
Eksenel periyodik sıcaklık
Kalın cidarlı borular
Üst akış bölgesine ısı geçişi

ÖZET

Kalın cidarlı borularda birleşik ısı transferi, eksenel ısı iletimi de dikkate alınarak incelenmiştir. Problem iki bölgeli sonsuz bir boruyu ele almaktadır. Borunun üst akış bölgesinde sabit dış duvar sıcaklığı sınır şartı varsayılmıştır. Alt akış bölgesinde dış duvar sıcaklığının eksenel yönde mekânsal olarak periyodik bir şekilde değiştiği kabul edilmiştir. Akışın laminer kabul edildiği bu problem sonlu farklar yöntemi ile sayısal olarak çözülmüştür. Cidar kalınlık oranı, Peclet sayısı, duvar-akışkan ısı iletkenlik katsayı oranı ve duvar-akışkan ısıl yayılım katsayı oranı temel parametrelerinin arayüz ısı akısı üzerindeki etkileri araştırılmıştır. Çalışmada eksenel boyutsuz frekansın sonuçlar üzerindeki etkileri ayrıca dikkate alınmıştır. Elde edilen sonuçlar büyük ölçüde parametrik değerlere bağlıdır. Özellikle cidar kalınlık oranının diğer parametrik değerlere nazaran daha etkili olduğu gözlemlenmiştir. Ayrıca boru cidarı ve akışkan eksenel iletiminin üst akış bölgesine ihmal edilemeyecek ölçekte ısı transferine neden olduğu söylenebilir.

ORCID ID: 0000-0002-5506-8200

***Corresponding author:** Sinop University, Faculty of Engineering and Architecture, Department of Mechanical Engineering, Sinop, Türkiye.
Tel: +90 555 4551559.
E-mail: aates@sinop.edu.tr

To cite this article: Ateş A., "Heat transfer in two-zone thick-walled pipes with axial varying periodic temperature boundary condition", Bozok Journal of Engineering and Architecture, vol. 3, no. 2, pp. 110-124, 2024.

1. INTRODUCTION

The periodic spatial variation of the outer surface temperature in pipes along the axial direction is different from the time-dependent periodic temperature variation boundary condition. Some examples related to this topic include oil or natural gas pipelines beneath wavy sea beds, heat exchangers in machines operating with the Stirling engine cycle, and cooling systems of nuclear reactors. Meanwhile, the analysis of transient conjugate heat transfer is also important for heat exchangers under conditions such as startup, shutdown, or changes in operating conditions. Transient heat transfer in pipes and channels with laminar flow has been investigated by some researchers. In most of the studies addressed, thin-walled pipes or channels were assumed where the conduction through the wall was neglected and the conditions on the outer surface were assumed to be directly applicable at the wall-fluid interface. However, in conjugate problems, since the boundary conditions at the interface are not known beforehand, energy equations must be solved simultaneously for both the wall and the fluid side, taking into account the temperature at the interface, the interfacial heat flux, and the continuity of the flow.

The problem of conjugate heat transfer in transient regimes has been examined in many studies [1, 2, 3] under conditions of sudden and periodic changes in boundary or inlet conditions, and some numerical solutions have been developed [4, 5].

Barletta et al. [6], investigated heat transfer between pipes used in offshore oil transportation and the environment. Conti et al. [7], examined the conjugate heat transfer problem in micro-channels for cases where the heat flux changes periodically and suddenly over time. [8], studied transient conjugate heat transfer under boundary conditions where the outer surface temperature of thick-walled pipes changes periodically over time.

Patankar et al. [9] found a method that obtains universal results in the fully developed region of periodic flows. Quaresma and Cotta [10] carried out an analytical study in which they obtained the temperature distribution and Nusselt Numbers in the thermal entrance region of pipes with variable wall heat flux in the axial direction. Barletta and Zanchini [11] conducted another study for hydrodynamically developed laminar flow through a thin-walled pipe where the ambient temperature varies periodically. Atmaca et al. [12] investigated the heat transfer in a thick-walled pipe partially heated circumferentially. Zniber et al. [13] carried out a study in which the temperature distribution and Nusselt numbers for periodically varying sinusoidal heat transfer boundary condition in Magneto-Hydrodynamic laminar flow were obtained using linear operators technique. Darici et al. [14] investigated the transient conjugate heat transfer for laminar flow developing simultaneously in a thick-walled semi-infinite pipe. Aydin and Avci [5,15] investigated the transient conjugate heat transfer in micro channels and channels with a periodically changing outer surface temperature boundary condition in the axial direction. Similar issues under different boundary conditions were also investigated by Zhu et al. [16].

In this study, transient conjugate heat transfer in a two-zone infinite pipe with a periodically changing outer surface temperature boundary condition in the axial direction depending on the position was investigated. In order to see the effects of axial conduction on both the pipe wall and fluid side, low Pe number flows in thick-walled pipes were emphasized.

2. MATERIALS and METHODS

2.1 Problem Definition

In this study, the transient conjugate heat transfer problem in a thick-walled pipe with laminar flow and thermal development region has been investigated. The effects of fluid axial conduction on heat transfer with two-dimensional conduction in the wall for flows with low Peclet numbers have been examined under a periodically varying surface temperature boundary condition. The schematic diagram of the problem and the coordinate system are shown in Figure 1.

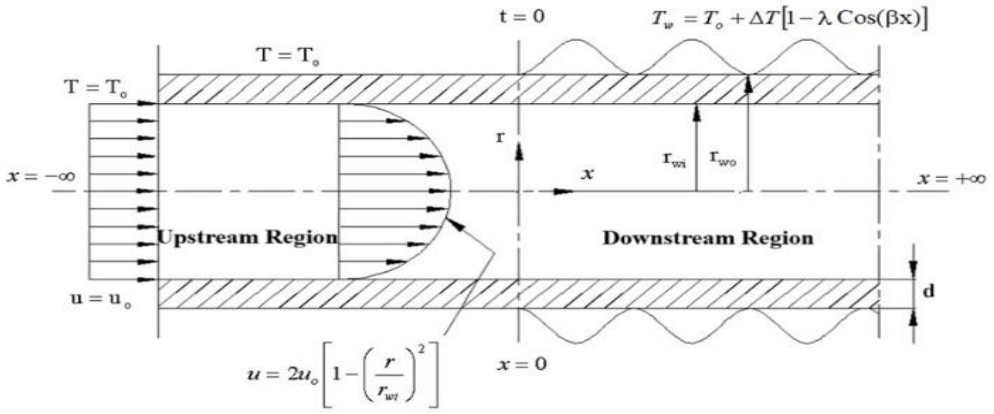

Figure 1. Coordinate system and diagram of the problem

As illustrated in the figure, the flow is considered as a two-region system, with the pipe being of infinite length in both directions. Far from upstream region (x =-∞), the fluid temperature is maintained at a constant uniform temperature, T_0. At position x=0 and at the beginning of time (t=0) downstream region of the pipe is exposed to the periodically varying the outdoor temperature, $T_w = T_o + \Delta T\left[1-\lambda \cos(\beta x)\right]$. All fluid and wall properties, density are assumed to be constant, and viscous dissipation is neglected. The flow is considered to be hydrodynamically developed, with the velocity distribution being independent of the temperature distribution.

2.2 Theoretical Fundamentals

In most fluid flow problems, the energy, continuity, and Navier-Stokes equations are solved together, simultaneously. Similar terms appearing in these equations must ensure consistency when substituted into the other equations. However, nonlinear terms in these differential equations significantly complicate the solution, sometimes rendering it impossible. Therefore, it becomes necessary to make assumptions that simplify complex expressions.

On the other hand, working with dimensionless forms of equations provides significant advantages in solving many problems. Converting differential equations to dimensionless form does not linearize a nonlinear equation. However, dimensional analysis is an ideal method for simplifying a complex equation with numerous variable expressions and parameters into a more manageable form. This approach also makes interpretations clearer.
Dimensionless parameters:

Dimensionless temperature; (for both wall and fluid)

$$T^* = \frac{T - T_{\min}}{T_{\max} - T_{\min}} = \frac{T - T_0}{T_w - T_0} \tag{1}$$

Axial coordinate;

$$x^* = \frac{x}{r_{wi} Pe} \equiv \frac{2}{Gz} \tag{2}$$

Radial coordinate;

$$r^* = \frac{r}{r_{wi}} \tag{3}$$

wall thickness;

$$d^* = \frac{d}{r_{wi}} \tag{4}$$

thermal conductivity coefficient ratio;

$$k_{wf} = \frac{k_w}{k_f} \tag{5}$$

thermal diffusivity coefficient ratio;

$$\alpha_{wf} = \frac{\alpha_w}{\alpha_f} \tag{6}$$

Dimensionless time;

$$t^* = \frac{t\ \alpha_f}{r_{wi}^2} \equiv Fo \tag{7}$$

Peclet number;

$$\mathrm{Pe} = \mathrm{Re}.\mathrm{Pr} = \frac{2u_0 r_{wi}\ \rho_f\ c_f}{k_f} \tag{8}$$

and dimensionless frequency;

$$F = Pe\beta r_{wi} \tag{9}$$

The dimensionless energy differential equation for the wall side is:

$$\frac{1}{\alpha_{wf}}\frac{\partial T_w^*}{\partial t'} = \frac{1}{r^*}\frac{\partial}{\partial r^*}\left(r^*\frac{\partial T_w^*}{\partial r^*}\right) + \frac{1}{Pe^2}\frac{\partial^2 T_w^*}{\partial x^{*2}} \tag{10}$$

Fluid side dimensionless energy differential equation is;

$$\frac{\partial T_f^*}{\partial t^*} + \left(1 - r^{*2}\right)\frac{\partial T_f^*}{\partial x^*} = \frac{1}{r^*}\frac{\partial}{\partial r^*}\left(r^*\frac{\partial T_f^*}{\partial r^*}\right) + \frac{1}{Pe^2}\frac{\partial^2 T_f^*}{\partial x^{*2}} \tag{11}$$

Nondimensionalization of wall side initial and boundary conditions;

For $t^* = 0$, $T_w^* = 0$ (12)

For $x^* = -\infty$, $T_w^* = 0$ (13)

For $x^* = +\infty$, $\frac{\partial T_w^*}{\partial x*} = \lambda F \,\mathrm{Sin}\left(F\, x^*\right)$ (14)

$r^* = 1 + d^*$ ve $x^* < 0$ için $T_w^* = 0$ (15)

For $r^* = 1 + d^*$ and $x^* \geq 0$, $T_w^* = \left[1 - \lambda \mathrm{Cos}\left(F\, x^*\right)\right]$ (16)

For $r^* = 1$, $T_w^* = T_f^*$ and also $\dfrac{\partial T_w^*}{\partial r^*} = \dfrac{1}{k_{wf}} \dfrac{\partial T_f^*}{\partial r^*}$ (17)

Nondimensionalization of initial and boundary conditions for the fluid side;

For $t^* = 0$, $T_f^* = 0$ (18)

For $x^* = -\infty$, $T_f^* = 0$ (19)

For $x^* = +\infty$, $\dfrac{\partial T_f^*}{x^*} = \lambda F \mathrm{Sin}\left(F\, x^*\right)$ (20)

For $r^* = 1$, $T_w^* = T_f^*$ and also $\dfrac{\partial T_f^*}{\partial r^*} = k_{wf} \dfrac{\partial T_w^*}{\partial r^*}$ (21)

for $r^* = 0$ (on the pipe axis) $\dfrac{\partial T_f^*}{\partial r^*} = 0$ (22)

The bulk temperature and heat flux at the interface can be expressed in dimensionless form as follows [1].

$$T_b^* = 4 \int_0^1 r^* \left(1 - r^{*^2}\right)\, T_f^*\, dr^* \tag{23}$$

$$q_{wi}^* = \frac{q_{wi}}{k_f \left(T_1 - T_0\right) / r_{wi}} \tag{24}$$

if defined as,

$$q_{wi}^* = -\left(\frac{\partial T_f^*}{\partial r^*}\right)_{r^*=1} \tag{25}$$

is obtained.

2.2 Numerical Solution

2.2.1 Discretization

To solve the problem using the finite difference method, the differential equations' initial and boundary conditions must be discretized. Discretization means that differential equations are expressed algebraically, in other words, solved numerically. In the equations, time-dependent terms are discretized using the fully implicit method, while the convection terms are discretized using the central difference method. Discretization has been carried out around the P point in a two-dimensional node system using Patankar's control volume approach [17].

For the wall side, discretization is performed for the control volume around the P point;

$$\frac{r_p^*}{\alpha_{wf}} \left(T_P^* - T^{0*}{}_P\right) \frac{\Delta x^* \Delta r^*}{\Delta t^*} = \left[r_n^* \frac{T_N^* - T_P^*}{(\delta r^*)_n} - r_s^* \frac{(T_P^* - T_S^*)}{(\delta r^*)_s}\right] \Delta x^* + \frac{r_P^*}{Pe^2} \left[\frac{T_E^* - T_P^*}{(\delta x^*)_e} - \frac{T_P^* - T_W^*}{(\delta x^*)_w}\right] \Delta r^* \tag{26}$$

is obtained. This equation can be compactly represented in computer notation as follows [18]:

$$a_P T_P^* = a_E T_E^* + a_W T_W^* + a_N T_N^* + a_S T_S^* + a_P^0 T_P^{0*} + c \tag{27}$$

$$a_E = \frac{r_p^* \, \Delta r^*}{Pe^2 (\delta x^*)_e} \tag{28}$$

$$a_W = \frac{r_p^* \, \Delta r^*}{Pe^2 (\delta r^*)_w} \tag{29}$$

$$a_N = \frac{r_n^* \, \Delta x^*}{(\delta r^*)_n} = \left[\frac{r_p^*}{(\delta r^*)_n} + 0.5 \right] \Delta x^* \tag{30}$$

$$a_S = \frac{r_s^* \, \Delta x^*}{(\delta r^*)_s} = \left[\frac{r_p^*}{(\delta r^*)_s} - 0.5 \right] \Delta x^* \tag{31}$$

$$a_P^0 = \frac{r_p^* \, \Delta x^* \, \Delta r^*}{\alpha_{wf} \Delta t^*} \tag{32}$$

$b=0$ and (33)

$c=0$ (34)

$$a_P = a_E + a_w + a_N + a_S + a_P^0 + b \tag{35}$$

The fluid side differential equation can be discretized around point P as;

$$r_p^* (T_P^* - T_P^{*0}) \, \frac{\Delta x^* \Delta r^*}{\Delta t^*} + (r_p^* - r_p^{*3}) \left\{ \left[T_P^* + \frac{T_P^* - T_E^*}{\exp\left[Pe^2 (1 - r_P^{*2}) \, (\delta x^*)_e \right] - 1} \right] - \left[T_W^* + \frac{T_W^* - T_P^*}{\exp\left[Pe^2 (1 - r_p^{*2}) (\delta x^*)_w \right] - 1} \right] \right\} \Delta r^* = \left[\frac{r_n^* (T_N^* - T_P^*)}{(\delta r^*)_n} - \frac{r_s^* (T_P^* - T_S^*)}{(\delta r^*)_s} \right] \Delta x^* \tag{36}$$

When this equation is written in compact form and the coefficients are determined,

$$a_P T_P^* = a_E T_E^* + a_W T_W^* + a_N T_N^* + a_S T_S^* + a_P^0 T_P^{0^*} + c \tag{37}$$

$$a_E = \frac{(r_P^* - r_P^{*3})}{\exp\left[Pe^2 (1 - r_P^{*2}) (\delta x^*)_e \right] - 1} \Delta r^* \tag{38}$$

$$a_W = \left(r_p^* - r_p^{*3} \right) \left\{ \frac{\exp\left[Pe^2 (1 - r_p^{*2}) (\delta x^*)_w \right]}{\exp\left[Pe^2 (1 - r_p^{*2}) (\delta x^*)_w \right] - 1} \right\} \Delta r^* \tag{39}$$

$$a_N = \frac{r_n^* \Delta x^*}{(\delta r^*)_n} = \left[\frac{r_p^*}{(\delta r^*)_n} + 0.5 \right] \Delta x^* \tag{40}$$

$$a_S = \frac{r_s^* \Delta x^*}{(\delta r^*)_s} = \left[\frac{r_p^*}{(\delta r^*)_s} - 0.5 \right] \Delta x^* \tag{41}$$

$$a_P^0 = \frac{r_p^* \Delta x^* \Delta r^*}{\Delta t^*} \quad (42)$$

$b=0$ and (43)

$c=0$ (44)

$$a_P = a_E + a_w + a_N + a_S + a_P^0 + b \quad (45)$$

is obtained.

Similar coefficients are determined for the initial and boundary conditions and written in their places in the equations.

2.2.2 Solution

The temperature distribution was determined and solved by the Gauss-Seidel iteration method using discretized equations. As a result of the precise and long experiments, 24 nodes were placed in the calculation region in the radial direction, 8 on the wall side and 16 on the fluid side. Similarly, it was found sufficient to place a total of 208 nodes in the axial direction for the upstream and downstream regions. The initial value of the axial step length was taken as 0.04. The initial value of the time step was taken as 0.005 and increased by 0.005 in each iteration step.

The convergence limit in the solutions was taken as 10^{-7} and the experiments in a time period were continued until the largest remaining mismatch in the control volume energy equations for all points fell below this value. When the total number of experiments for a time period fell below 2, the system was considered to have reached the steady state and the experiments were terminated.

3. RESULTS and DISCUSSION

In this numerical study, four dimensionless parameters have been considered. These parameters are: wall thickness ratio d', Peclet Number Pe, wall-fluid thermal conductivity ratio k_{wf}, and wall-fluid thermal diffusivity ratio α_{wf}. The average values of these parameters and their different combinations have been analyzed in relation to the dimensionless frequency F. Initially, results are presented for an F value corresponding to a full period (for F=6.3), and later for larger F values. In selecting the average parametric values, conditions that could significantly reflect scenarios encountered in practical engineering applications have been considered. Given the wall thicknesses that might be encountered in microtubes, this study specifically selected large values for wall thicknesses. A graph including different wall thicknesses has also been provided.

In similar studies of this type, results are typically examined in terms of the local Nusselt number. However, in conjugate heat transfer problems, due to the high number of unknowns in the Nusselt number formulation, it is not very suitable to present results based on the Nu number [19, 20]. Therefore, in this study, results are generally presented in relation to the heat flux at the interface q_{wi}, which provides more illuminating insights. Additionally, some results have been presented in terms of the interface temperature and the fluid bulk temperature. Presenting the results in this way is an accepted convention in the literature [3, 14, 18].

Figure 2 shows the variation of the interface heat flux in the axial direction at different time intervals for a combination of average parameter values such as Pe=4, d*=0.6, k_{wf}=1 and α_{wf}=0.1. Here, F = 6.3 has been selected to be close to a full period value. Figures 3, 4, and 5 provide the variation graphs of the outer surface, interface, and fluid bulk temperatures with respect to the axial position for the same values. The curves for this specific dimensionless frequency are provided primarily to allow comparison with other figures.

Figure 2 shows that at the beginning of time, the interface heat flux values oscillate entirely within the positive region. The wave amplitude is small because the sinusoidal temperature variation at the outer surface has only just begun to show its effect. As time progresses, both the sinusoidal wave height increases and the interface heat flux values alternate between the positive and negative regions. In other words, local axial heat transfer occurs in the reverse direction from the tube to the fluid and from the fluid to the tube. At the onset of the event, the sudden change in the outer surface temperature causes a sharp increase in heat transfer values, which then stabilizes into a steady state.

Figure 3 is provided to illustrate the alternating variation of the outer surface temperature over a full period.

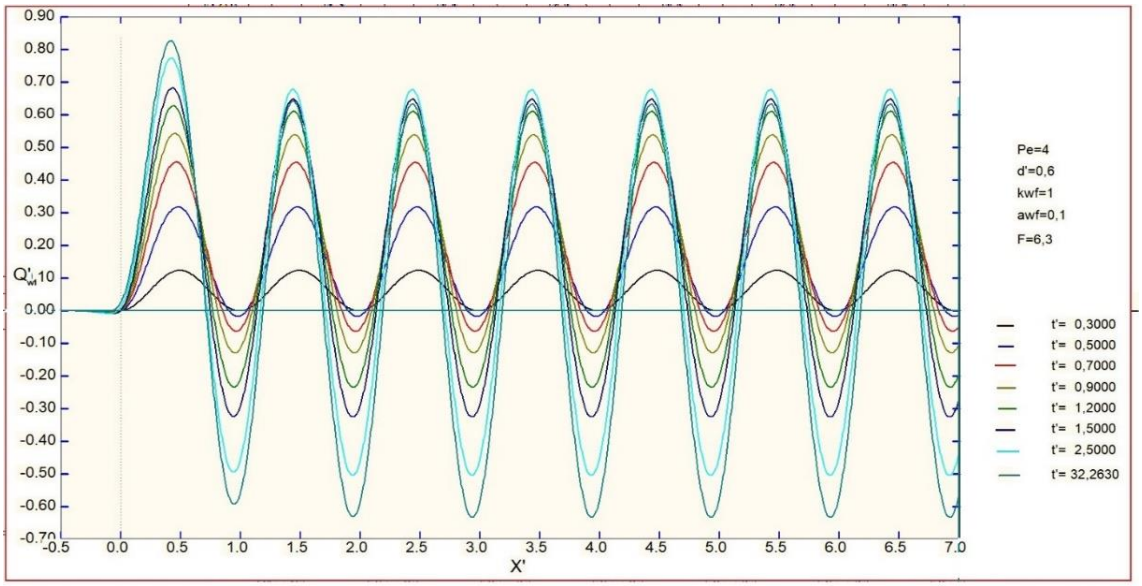

Figure 2. Transient axial distribution of interfacial heat flux (F=6.3)

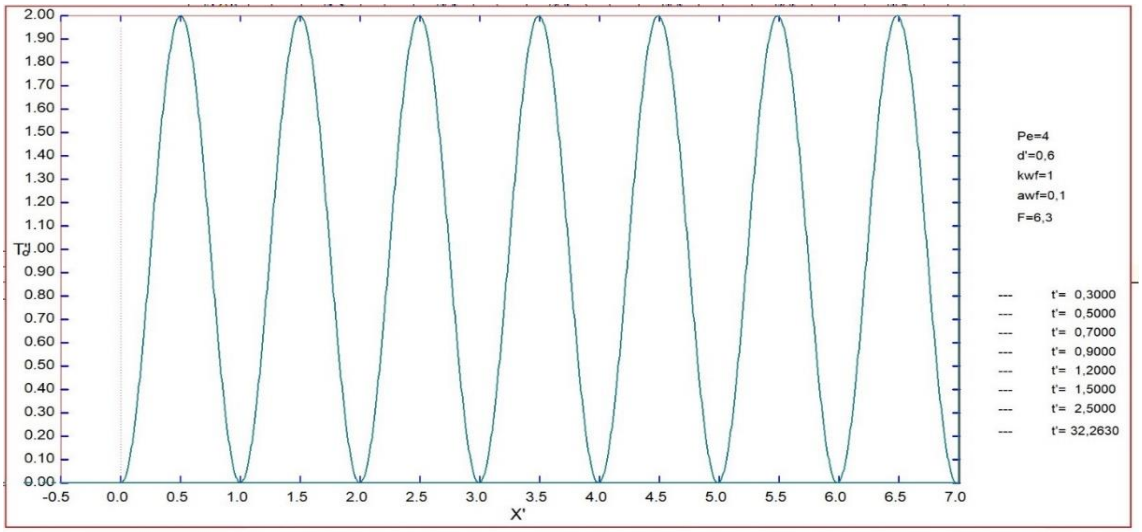

Figure 3. Transient axial distribution of outer surface temperature (F=6.3)

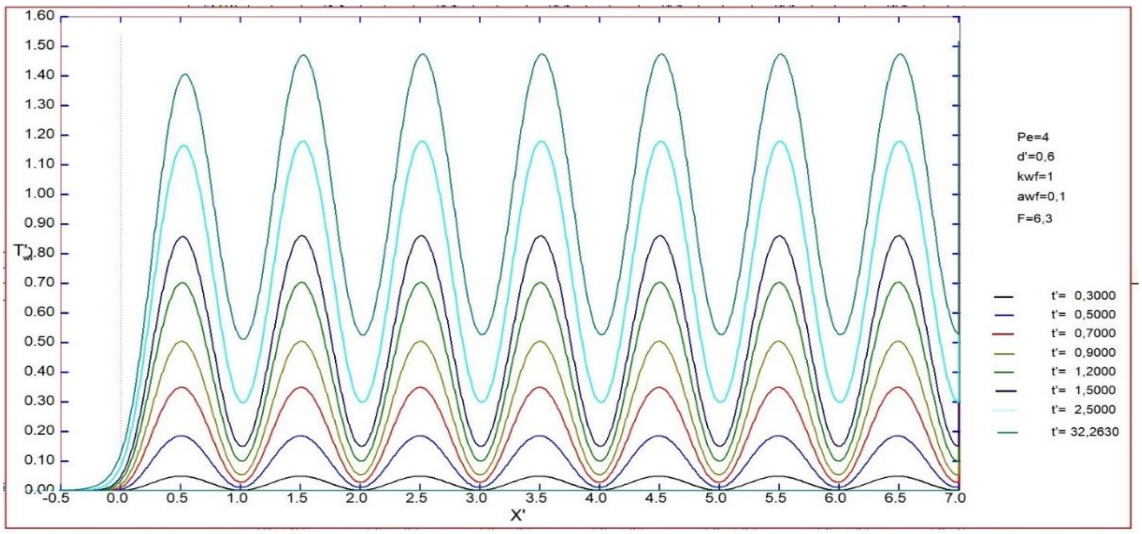

Figure 4. Transient axial distribution of interface temperature (F=6.3)

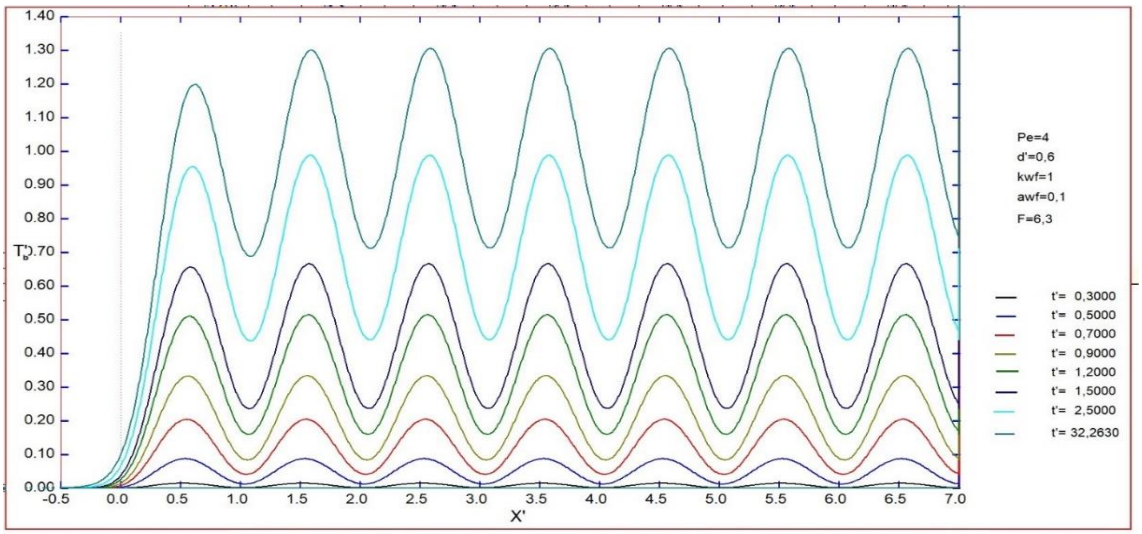

Figure 5. Transient axial distribution of bulk temperature (F=6.3)

Figure 4 is a good indicator of how the interface temperature evolves over time in relation to the outer surface temperature. In the steady state, although the peak temperature at the beginning of the axial position is slightly lower, it reaches a stable peak value at later positions before entering a downward trend. This is because the temperature will stabilize both over time and with progressing position.

A similar situation is observed in the bulk temperature curve in Figure 5. At the initial position, the peak value is lower, but at later positions, it remains at a stable peak in the steady state. However, these peak values are lower than the peak values of the interface temperature.

A common feature across all figures from Figure 2 to Figure 10 is that the time to reach the steady state is the same. The average parametric values, including the Peclet number, wall thickness ratio, thermal conductivity ratio, and thermal diffusivity ratio, are consistent in these figures. Therefore, the change in frequency does not affect the time to reach the steady state.
In Figure 6, the interface heat flux curves for a dimensionless frequency value of 150 are shown. These curves indicate that just before the beginning of downstream region, moving to the left from x'=0, there is a negative heat flux, meaning heat is transferred from the fluid to the tube. This suggests that at the beginning of downstream region, heating affects upstream region, resulting in a heat flux towards upstream region. At low Peclet numbers and high wall thickness values, heat transfer values to upstream region, or backward heat transfer, are higher [1, 2, 14]. At low Peclet numbers, axial heat conduction within the fluid is significant, which leads to pre-heating of the fluid and an increase in temperature to values higher than the initial temperature T_0. As a result, heat is transferred from the fluid to the tube. Similarly, a thicker tube wall causes backward heat flux due to the effect of wall axial conduction. This also causes the temperature to rise to values higher than T_0 and results in reverse heat flux.

Another notable aspect in Figure 6 is the sudden increase in the interface heat flux values at the beginning of downstream region. At the early stage of the event, the temperature difference is larger, leading to rapid heat transfer. Consequently, the heat flux initially increases. However, as one progresses in the axial direction, the fluctuations in the interface heat flux stabilize into a steady state.
The difference between Figure 4 and Figure 7 is quite evident. As the frequency increases, the oscillations in the interface temperature curves become quicker and the wavelengths shorter. This is expected because with higher frequency, the temperature starts rising again before dropping to lower values, making the periodic oscillation process faster. Therefore, the sinusoidal temperature wave has a shorter amplitude.

The same observations can be applied to Figure 9. In Figure 9, the wave amplitude is much shorter because the influence of the outer surface temperature lasts longer, even though the axial distance remains the same. The more pronounced effects of Figures 7 and 8 are seen in Figures 9 and 10. In these two figures, the dimensionless frequency value is quite high, and the temperature curves are almost straight lines. As such, Figures 9 and 10 are in significant agreement with the results from the study by Ates et al. [2].

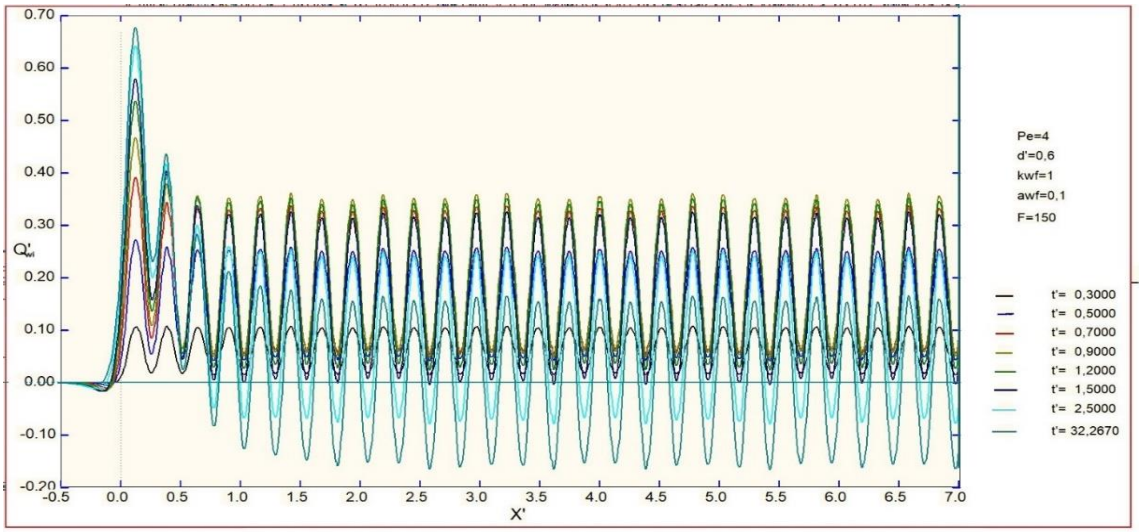

Figure 6. Transient axial distribution of interfacial heat flux (F=150)

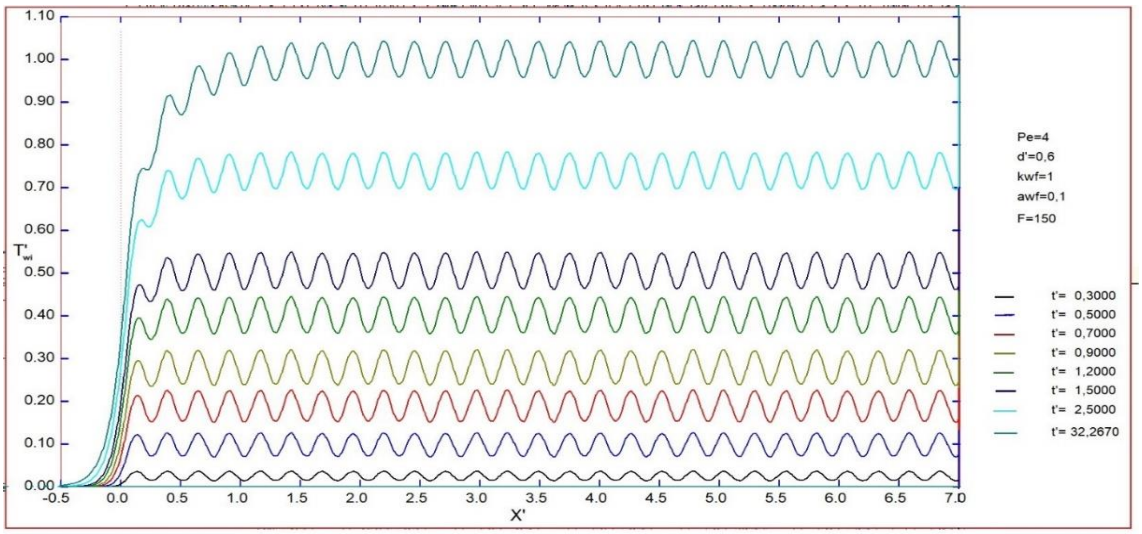

Figure 7. Transient axial distribution of interface temperature (F=150)

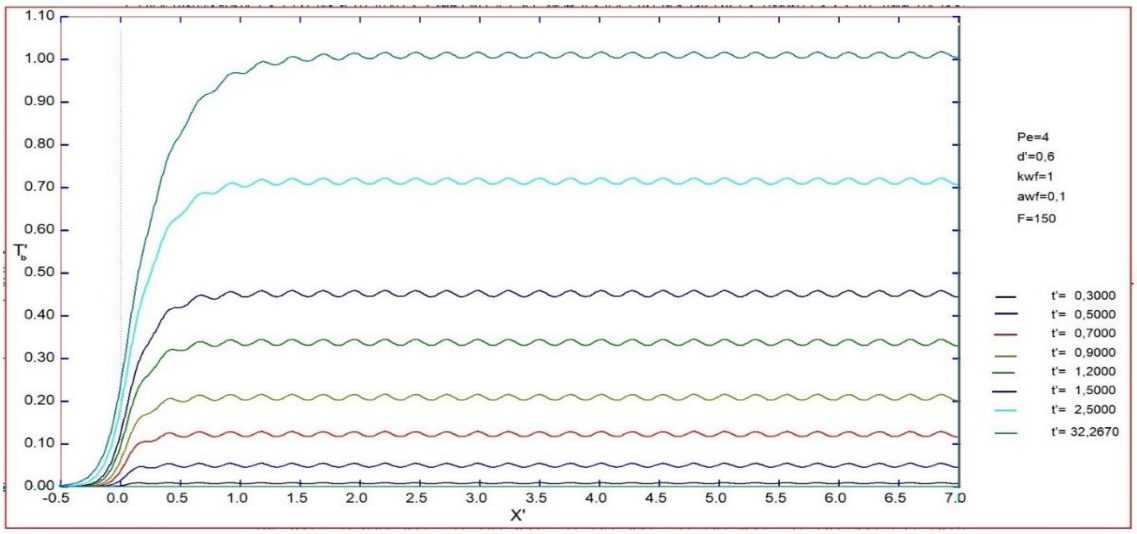

Figure 8. Transient axial distribution of bulk temperature (F=150)

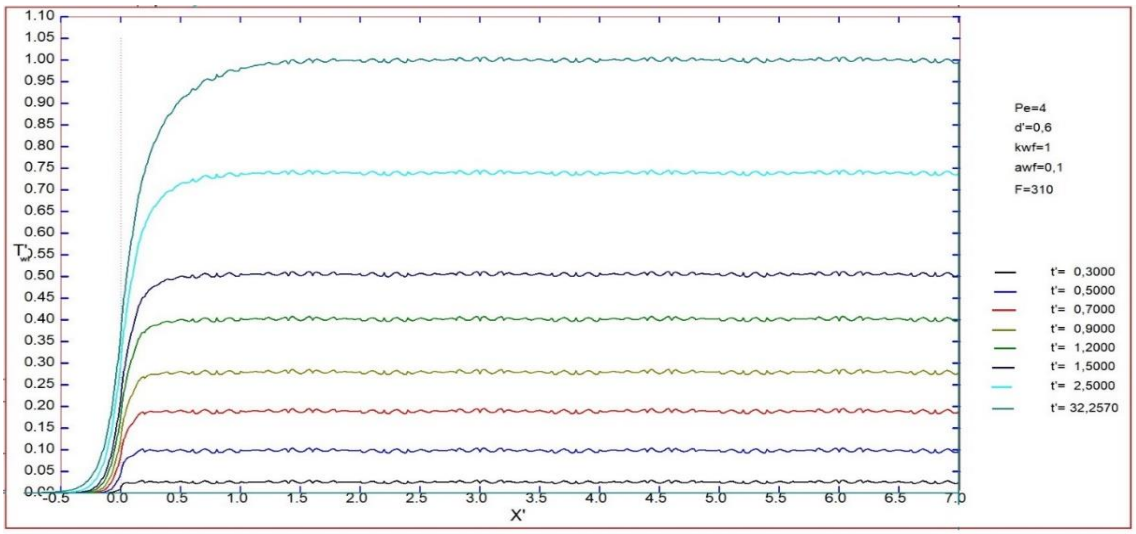

Figure 9. Transient axial distribution of interface temperature (F=310)

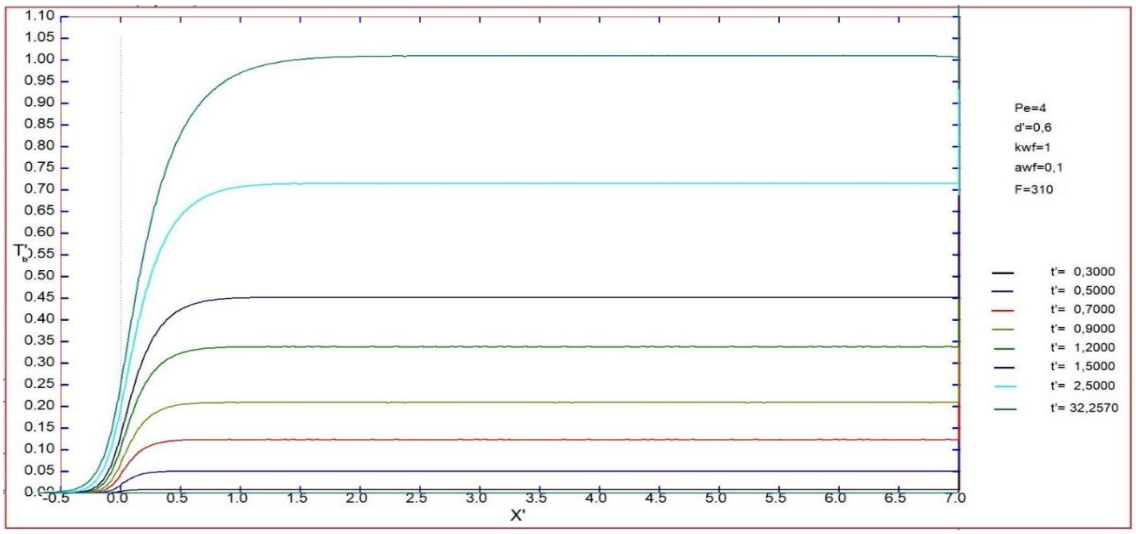

Figure 10. Transient axial distribution of bulk temperature (F=310)

Figure 11 shows the effect of wall thickness ratio on the interface heat flux. Here, the wall thickness ratios are selected to be quite large. In microtubes, the wall thickness is generally very high relative to the tube diameter, resulting in a large ratio of wall thickness to the inner radius. Therefore, wall thickness ratios are chosen to be large to resemble applications in microtubes. What stands out in the figure is the significant level of heat transfer from downstream region to upstream region at the beginning. For small wall thickness ratios, there is initially negative heat transfer, meaning from the fluid to the wall. For large wall thickness ratios, positive but more extensive and further backward heat transfer is observed. Although a peak in heat flux is visible at the entrance due to the high ΔT temperature difference at the beginning of downstream region, the heat flux values in the positive and negative regions equalize in the steady state. Thus, the total heat transfer from the wall becomes zero.

Figure 12 shows the effect of wall thickness ratio on the interface heat flux at high frequency values. For x'=0, the left and right sides show some minor differences, but similar observations to those in the previous figure can be made. What is striking here is the difference between small and large wall thickness ratios. For small wall thickness ratios, heat transfer occurs in a sinusoidal form, while for large wall thickness ratios, the wave amplitude decreases rapidly and eventually becomes zero after a certain value (e.g., d'=1.5 and d'=2). In other words, no heat transfer occurs into or out of the surface.

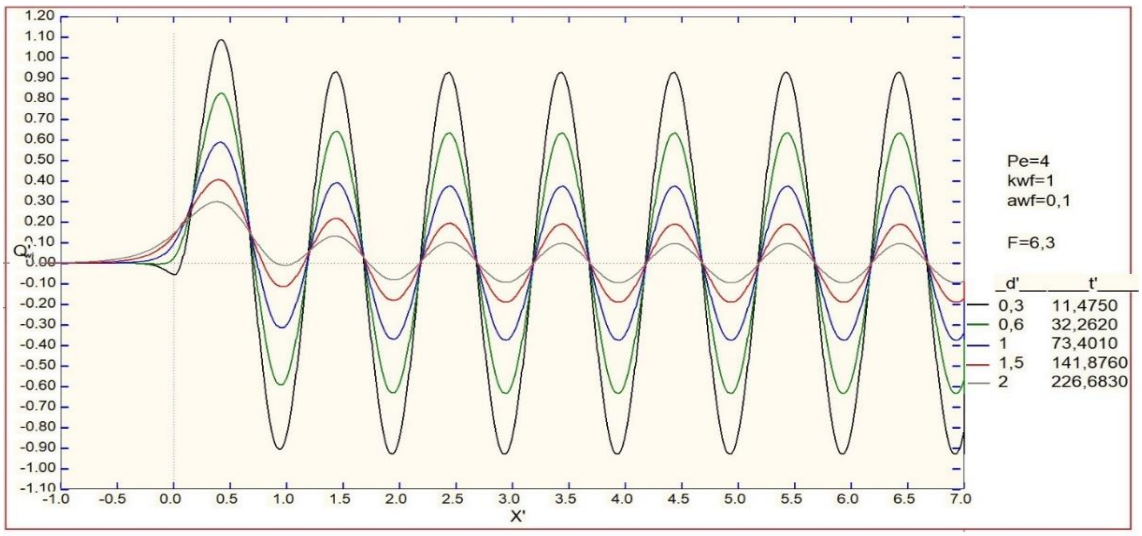

Figure 11. Change of interface heat flux with wall thickness ratio (for F=6,3)

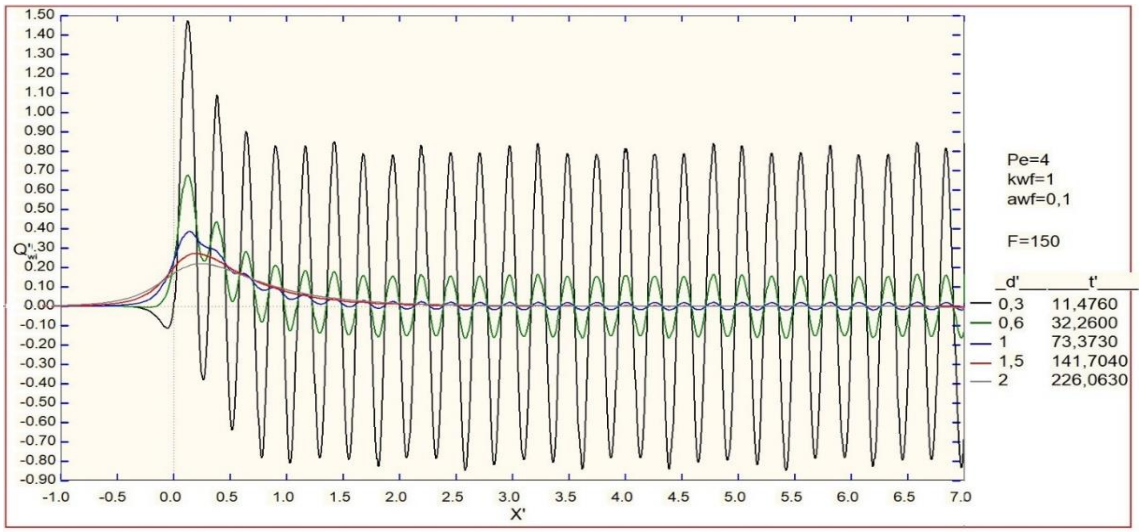

Figure 12. Change of interface heat flux with wall thickness ratio (for F=150)

4. CONCLUSION

The transient regime of conjugate heat transfer in the thermal entrance region of a thick-walled, infinitely long pipe with laminar flow has been examined, taking into account the axial conduction in the fluid. The pipe has been divided into two regions: upstream region and downstream region. While the outer surface of upstream region is maintained at a constant temperature, downstream region is exposed to a periodically varying temperature effect in the axial direction from its beginning. The problem was solved numerically using the finite difference method. The effects of four independent parameters were investigated in the problem. These parameters are: the wall thickness ratio d', the wall-fluid thermal conductivity ratio k_{wf}, the wall-fluid thermal diffusivity ratio α_{wf} and the Peclet number. The problem was solved for different values of the dimensionless frequency F of the periodic temperature variation. The obtained results can be summarized as follows:

1. Axial Conduction and Pre-heating: Due to axial conduction on both the wall and fluid sides, a significant amount of heat is transferred to upstream region. This reverse heat diffusion increases the temperature in the heated lower flow region and results in pre-heating of the unheated upper flow region. This pre-heating effect is more pronounced for $F > 6$.

2. Reverse Heat Transfer: The tendencies for interface and bulk temperatures to spread towards $x'<0$, i.e., towards upstream region, are less when F is small and become greater as F increases. For example, the heat transfer to the $x<0$ region is more pronounced in Figure 6 than in Figure 2. However, beyond a certain value of F, this spreading remains constant.

3. Periodic Variation: The interface heat transfer varies periodically in response to changes in the outer wall temperature. The amplitudes of these variations are strongly dependent on parameter values and frequency. However, the average is generally zero.

4. Effect of Parameters: The effects of conjugate heat transfer and fluid axial conduction increase as the pipe wall thickness ratio (d') increases and as k_{wf}, α_{wf} and the Peclet number decrease. Beyond certain values, the effects of these parameters and frequency become negligible. Parameter values also affect the thermal development length and the time to reach a steady state. As the wall thickness ratio increases, the time to reach a steady state significantly lengthens.

5. Fully Developed Region: In the fully developed and steady-state regions, the average interface temperature is 1.0, while the average bulk temperature is slightly lower. The average of the interface heat flux and, therefore, the net heat transfer from the pipe wall to the fluid is zero in the fully developed and steady state. This results in pre-heating of the fluid before this region. The amount of preheating and the length of penetration increase over time and go backwards.

The graphs and results obtained from this study can be reproduced by applying different values of various parameters such as the Peclet number, the thermal conductivity ratio, and the thermal diffusivity ratio. Additionally, working with different values of the dimensionless frequency F will lead to interesting results. Developing a new mathematical model and formulation for nanofluids and compressible flows could further elevate the study to a different level.

REFERENCES

[1] S. Bilir, and A. Ates, "Transient conjugated heat transfer in thick walled pipes with convective boundary conditions." International Journal of Heat and Mass Transfer, 46(14): 2701–2709, 2003, https://doi.org/10. 1016/S0017-9310(03)00032-2

[2] A. Ates, S. Darici, and S. Bilir, "Unsteady conjugated heat transfer in thick walled pipes involving two-dimensional wall and axial fluid conduction with uniform heat flux boundary condition", International Journal of Heat and Mass Transfer, 53(23–24): 5058–5064, 2010, https://doi.org/10.1016/j.ijheatmasstransfer.2010.07.059

[3] A. Ateş, "Transient conjugated heat transfer in thick walled pipes with axially periodic surface temperature in downstream region", Sādhanā, 44, 82, 2019. https://doi.org/10.1007/s12046-019-1079-z

[4] A. Barletta, E. Rossi di Schio, "Effects of viscous dissipation on laminar forced convection with axially periodic wall heat flux", Heat and Mass Transfer, 35: 9–16, 1999. https://doi. org/10.1007/s002310050292

[5] O. Aydın, and M. Avcı, "Laminar forced convective slip flow in a microduct with a sinusoidally varying heat flux in axial direction", International Journal of Heat and Mass Transfer, 89:606–612, 2015, https://doi.org/10.1016/j.ijheatmasstransfer. 2015.05.056

[6] A. Barletta, E. Rossi di Schio, G. Comini, and P. D'Agaro, "Wall coupling effect in channel forced convection with streamwise periodic boundary heat flux variation", International Journal of Thermal Science, 48: 699–707, 2009. https://doi.org/10.1016/j.ijther malsci.2008.06.003.

[7] A. Conti, G. Lorenzini, and Y. Jaluria, "Transient conjugate heat transfer in straight microchannels", International Journal of Heat and Mass Transfer, 55: 7532–7543, 2012, https://doi.org/10.1016/j.ijheatmas stransfer.2012.07.046

[8] A. H. Altun, S. Bilir, and A. Ates, "Transient conjugated heat transfer in thermally developing laminar flow in thick walled pipes and minipipes with time periodically varying wall temperature boundary condition", International Journal of Heat and Mass Transfer, 92: 643–657, 2016, https://doi.org/10.1016/j.ijheatmas stransfer.2015.09.011.

[9] S. V. Patankar, C. H. Liu, and E. M. Sparrow, "The periodic thermally developed regime in ducts with streamwise periodic wall temperature or heat flux", International Journal of Heat and Mass Transfer, 21: 557–565, 1978, https://doi.org/10.1016/0017-9310(78)90052-2.

[10] J. N. N. Quaresma, and R. M. Cotta, "Exact solutions for thermally developing tube flow with variable wall heat flux", International Communication Heat and Mass Transfer, 21(5): 729–742, 1994, https://doi.org/10.1016/0735-1933(94)90074-4

[11] A. Barletta, and E. Zanchini, "Laminar forced convection with sinusoidal wall heat flux distribution: axially periodic regime", Heat & Mass Transfer, 31: 41–48, 1995, https://doi.org/10. 1007/BF02537420.

[12] U. Atmaca, S. Bilir, and A. Ates, "Effects of wall conjugation and fluid axial conduction in circumferentially partly heated pipes and minipipes", Heat Transfer Research, 48(16): 1433–1458, 2017, https://doi.org/10.1615/heattransres.2017017830

[13] K. Zniber, A. Oubarra, and J. Lahjomri, "Analytical solution to the problem of heat transfer in an MHD flow inside a channel with prescribed sinusoidal wall heat flux", Energy Conversation Management, 46: 1147–1163, 2005. https://doi.org/10.1016/j.enconman. 2004.06.023

[14] S. Darici, S. Bilir, and A. Ates, "Transient conjugated heat transfer for simultaneously developing laminar flow in thick walled pipes and minipipes", International Journal of Heat and Mass Transfer, 84: 1040–1048, 2015, http://dx.doi.org/10.1016 /j.ijheatmasstransfer.2014.12.049

[15] O. Aydin, M. Avci, T. Bali & M. E. Arıcı, "Conjugate heat transfer in a duct with an axially varying heat flux", International Journal of Heat and Mass Transfer, 76: 385–392, 2014. https://doi.org/10.1016/j. ijheatmasstransfer.2014.04.062.

[16] X. W. Zhu, Y. H. Fu, and J. Q. Zhao, "A novel wavy-tape insert configuration for pipe heat transfer augmentation", Energy Conversatiton Management, 127: 140–148, 2016, https://doi.org/10. 1016/j.enconman.2016.09.006

[17] S. V. Patankar, Chapter 4 "Numerical heat transfer and fluid flow", In: W J Minkowycz and A M Sparrow (eds), Newyork: Hemisphere Publishing Corporation, McGraw-Hill Book Company, pp. 44–47, 1980.

[18] A. Ates, "Transient conjugated heat transfer in thick walled pipes with convective boundary conditions". Ph.D. Thesis. Selcuk University, Konya, Turkey, 1998.

[19] M. Faghri, and E. M. Sparrow, "Forced convection in a horizontal pipe subjected to nonlinear external natural convection and to external radiation", International Journal of Heat and Mass Transfer, 23(6): 861–872, 1980, https://doi.org/10.1016/0017-9310(80)90041-1.

[20] D. J. Schutte, M. M. Rahman and A. Faghri, "Transient conjugate heat transfer in a thick walled pipe with developing laminar flow. Numer", Heat Transf. Part A Applications, 21: 163–186, 1992, https://doi.org/10.1080/10407789108944871

List of symbols

a	constant of discretization equation
c_p	specific heat at constant pressure, (kJ/kgK)
d	thickness of the pipe wall, (m)
F	dimensionless frequency
Fo	Fourier number
Gz	Graetz number
k	thermal conductivity, (W/mK)
P	order of computational method
Pe	Peclet number
q	heat flux, (W/m2K)
r	radial coordinate, (m)
Re	Reynolds number
t	time, (s)
T	temperature, (K)
To	initial temperature of the system, (K)
u	axial velocity, (m/s)
x	axial coordinate, (m)

Greek symbols

α	thermal diffusivity, (m2/s)
β	frequency, (Hz)
dr	radial position difference
dx	axial position difference
Δr	radial step size, (m)
Δt	time step increment, (s)
ΔT	amplitude of periodic temperature variation, (K)
Δx	axial step size, (m)
λ	Wavelength (m)

Subscripts

b	bulk
c	coarse
f	fluid
i	inner wall
i, j	at nodal point i, j

m	mean
max	maximum
o	outer wall
w	wall
wf	ratio of wall to fluid
wi	wall to fluid interface

Superscripts

*	dimensionless quantity
0	at previous time step